

Simple model for inhomogeneous mixed-valence systems: Application to Sm_3S_4 and Eu_3S_4

J. L. Morán-López* and P. Schlottmann

Institut für Theoretische Physik, Freie Universität Berlin 1000 Berlin 33, Arnimallee 3, Germany

(Received 17 December 1979)

A simple model to describe the transport and magnetic properties of semiconducting inhomogeneous mixed-valence systems is presented. We assume that there is a nearest-neighbor charge interaction between the divalent and trivalent rare-earth ions and that there is a nearest- and next-nearest-neighbor Ising-type interaction among the magnetic moments. The magnetic and the charge order are studied within the Bethe-Peierls approximation. Depending on the coupling parameters the ground state of the system might be ferromagnetic charge ordered, antiferromagnetic charge ordered, segregated (clusters of ions with the same valence) ferromagnetic, and segregated antiferromagnetic. The observed discontinuity of the conductivity in Sm_3S_4 is explained in terms of an order-disorder transition.

I. INTRODUCTION

Mixed-valence compounds are systems in which the cations are present in more than one valence state, e.g., the $4f^n$ and $4f^{n-1}5d$ configurations of rare earth (R) ions. It is useful to distinguish between homogeneous and inhomogeneous mixed-valence compounds. In the former case¹ localized and band states coexist hybridized near the Fermi surface and a metalliclike conductivity is observed. In the case of inhomogeneous mixed-valence compounds² the ionic configurations are frozen since there are no extended states at the Fermi level and the transport properties are like those of a semiconductor. These systems are further classified² according to whether the cation sites are equivalent, as for Sm_3S_4 and Eu_3S_4 , or inequivalent as for example for Eu_3O_4 and Fe_3O_4 .

In this paper we present a simple model for inhomogeneous mixed-valence systems with equivalent cation sites and apply it to $R_3\text{S}_4$ ($R = \text{Sm}, \text{Eu}$). These compounds crystallize in the Th_3P_4 structure, where the R ions form a bcc lattice,³ and are n -type semiconductors⁴ with a high carrier density of 10^{21} cm^{-3} . Divalent and trivalent R ions are present in the ratio 1:2, such that the average R valence is 2.66 and one can write the net formula²⁻⁴ as $R^{2+}R_2^{3+}S_4^{2-}$. The energy-level diagram as obtained by electrical and optical measurements² shows that the $3p^6$ -valence states of S are far below the $6s$ $5d$ conduction band and do not play any further role. The ground states of the $4f^6$ configuration of Sm^{2+} and of the $4f^5$ configuration of Sm^{3+} are below the bottom of the conduction band by about 0.2 and 5 eV, respectively. Hence the $6s$ $5d$ conduction band is empty and can be neglected as a first approximation.

The valence fluctuations are due to thermally activated hopping²⁻⁴ of the $4f$ electrons. The hopping frequency is given by

$$\nu = \nu_0 e^{-\Delta E/T}, \quad (1.1)$$

where ν_0 is of the order of $4 \times 10^{13} \text{ sec}^{-1}$ and $\Delta E \approx 0.14 \text{ eV}$.^{2,3,5} The conductivity data² for Sm_3S_4 shows a change in the activation energy at 125 K, which is attributed to the formation of a long-range charge order. The Mössbauer spectra^{5,6} for Eu_3S_4 are also consistently interpreted in terms of a thermally activated hopping.

Since the spatial configuration of the $4f$ electrons is essentially frozen at low temperatures one expects the system to order magnetically. The Mössbauer data⁶ revealed that Eu_3S_4 is ferromagnetically ordered below $T_c = 3.8 \text{ K}$. The situation is not so clear for Sm_3S_4 . Extrapolating the bulk measurements⁷ of χ for Sm_3S_4 to low temperatures, a Néel temperature of 1 K corresponding to antiferromagnetic order is obtained. In contrast to the above result there is a previous measurement⁸ which shows a Pauli-type susceptibility, ruling out a magnetic ordering and the existence of the magnetic moments of Sm^{3+} .

Our model involves only $4f$ electrons and we neglect their orbital degeneracy. Since the hopping frequency is much smaller than the charge interaction between the divalent and trivalent R ions, we assume that the thermodynamical properties of the system are not affected by the dynamics of the $4f$ electrons. The compound can thus be considered as an alloy of R^{2+} and R^{3+} ions. Concerning the magnetic moments of Eu^{2+} and Sm^{3+} we assume that they can have only the two orientations up and down, i.e., we replace them by a spin $\frac{1}{2}$. This represents a considerable simplification of the calculation.

We introduce a nearest-neighbor charge interaction between the divalent and trivalent R ions, which takes account for their difference in size and charge. We further consider a nearest- and next-nearest-neighbor spin interaction of the Ising type. The thermodynamical properties are discussed within the Bethe-Peierls approximation.⁹ Depending on the signs and strengths of the

interaction parameters the ground state of the system might be ferromagnetic charge ordered, antiferromagnetic charge ordered, ferromagnetic with ions of the same valence clustered (segregation), and segregated antiferromagnetic.

By determining the strength of the charge interaction with the transition temperature $T_c = 125$ K, we obtain a change in the activation energy for the conductivity of Sm_3S_4 , which is in good agreement with the experimental data,² without adjusting other parameters.

The rest of the paper is organized as follows. The model is described in Sec. II. In Sec. III we calculate the phase diagram at $T = 0$, the transition temperatures to the ordered phases and the conductivity of Sm_3S_4 near the order-disorder transition, as well as the discontinuity of the specific heat at the transition. We close the paper with a summary and a brief discussion of the results (Sec. IV).

II. THE MODEL

As mentioned in the introduction only f electrons play a role and their dynamics can be neglected in thermodynamical properties. For the sake of simplicity we replace the $S = \frac{7}{2}$ of the Eu^{2+} ions and the $J = \frac{5}{2}$ of the Sm^{3+} by a spin $\frac{1}{2}$ with a correspondingly enhanced magnetic moment. The system can now be considered as a ternary alloy consisting of Sm^{3+} (Eu^{2+}) ions which may have spin up or down and Sm^{2+} (Eu^{3+}) ions without magnetic moment.¹⁰

The R ions are on a bcc lattice.³ We introduce two sublattices α and β , such that each ion of one sublattice is surrounded by z sites of the other sublattice, z being the coordination number. We limit ourselves to a probabilistic description of the local environment by defining bond probabilities of nearest-neighbor pairs. Denoting the three alloy components by + (spin up), - (spin down), and 0 (no spin) we introduce the pair probabilities $P_{ij}^{\alpha\beta}$ (where i, j take the values +, -, 0) giving the probability of finding an ion i at the site α and an ion j at the site β . There are nine pair probabilities, normalized by the condition

$$\sum_{ij} P_{ij}^{\alpha\beta} = 1. \quad (2.1)$$

The single-site probabilities expressed in terms of the $P_{ij}^{\alpha\beta}$ are given by

$$n_i^\alpha = \sum_j P_{ij}^{\alpha\beta}, \quad n_j^\beta = \sum_i P_{ij}^{\alpha\beta}, \quad (2.2)$$

where n_i^α denotes the probability of finding the alloy component i at the site α . The probabilities are further constrained by the total number of

electrons, i. e.,

$$\frac{1}{2}(n_0^\alpha + n_0^\beta) = \frac{2}{3} = x \quad \text{for } \text{Eu}_3\text{S}_4 \quad (2.3a)$$

and

$$\frac{1}{2}(n_0^\alpha + n_0^\beta) = \frac{1}{3} = x \quad \text{for } \text{Sm}_3\text{S}_4. \quad (2.3b)$$

These relations determine the concentration x of nonmagnetic Eu^{3+} ions and Sm^{2+} ions, respectively.

Within the pair approximation the entropy of the system is given by^{9,10}

$$S = \frac{N}{2}(z-1) \sum_i (n_i^\alpha \ln n_i^\alpha + n_i^\beta \ln n_i^\beta) - N \frac{z}{2} \sum_{ij} P_{ij}^{\alpha\beta} \ln P_{ij}^{\alpha\beta}, \quad (2.4)$$

where N is the total number of R sites.

As mentioned above we consider a charge (chemical) interaction between nearest-neighbor ions and an Ising-type interaction between nearest and next-nearest neighbors.

The chemical interaction is due to the difference in size and charge of divalent and trivalent R ions. The internal energy associated with it can be written as

$$H_c = NzU(P_{++}^{\alpha\beta} + P_{+-}^{\alpha\beta} + P_{-+}^{\alpha\beta} + P_{--}^{\alpha\beta} + P_{00}^{\alpha\beta} - P_{+0}^{\alpha\beta} - P_{-0}^{\alpha\beta} - P_{0+}^{\alpha\beta} - P_{0-}^{\alpha\beta}) + \text{const.} \quad (2.5)$$

The above combination of pair probabilities corresponds to the probability of finding a pair of R ions with the same charge minus the probability of having a pair with different charges. Here, $U = U_{++} + U_{00} - 2U_{0+}$, and U_{ij} is the effective interaction between the i and j ions. We define the chemical short- and long-range order parameters σ and η by

$$\sigma \equiv 1 - \frac{1}{2x(1-x)} (P_{+0}^{\alpha\beta} + P_{-0}^{\alpha\beta} + P_{0+}^{\alpha\beta} + P_{0-}^{\alpha\beta}) \quad (2.6)$$

and

$$\eta \equiv P_{+0}^{\alpha\beta} + P_{-0}^{\alpha\beta} - P_{0+}^{\alpha\beta} - P_{0-}^{\alpha\beta}. \quad (2.7)$$

The energy H_c depends only on σ and can be written as

$$H_c = 4NzUx(1-x)\sigma + \text{const.} \quad (2.8)$$

Note that for our systems $U > 0$, since the interaction is repulsive of the Coulomb type or, equivalently, it can be interpreted as of elastic nature (ion-size effect).

The nearest-neighbor spin interaction can be written as

$$H_{M1} = -NzS^2J_1(P_{++}^{\alpha\beta} + P_{--}^{\alpha\beta} - P_{+-}^{\alpha\beta} - P_{-+}^{\alpha\beta}), \quad (2.9)$$

where S is the spin of the R ions. There are two main competing mechanisms contributing to the spin interaction: the superexchange,¹¹ which is always antiferromagnetic, and the indirect exchange¹¹

via the $5d$ band, which is always ferromagnetic. Both mechanisms are short ranged and depending on which one dominates the net interaction, may be ferromagnetic ($J_1 > 0$) or antiferromagnetic ($J_1 < 0$).

In order to include a next-nearest-neighbor interaction among the spins we express the probabilities of next-nearest-neighbor pairs in terms of the $P_{ij}^{\alpha\beta}$. Next-nearest-neighbor sites belong to the same sublattice. Assuming that the nearest-neighbor bonds are all independent we obtain for the probability of finding a next-nearest-neighbor pair i, l in the α sublattice

$$\sum_j \frac{P_{ij}^{\alpha\beta} P_{li}^{\alpha\beta}}{n_j} \quad (2.10)$$

Summing over i and l these probabilities are normalized to one. The probabilities in the β sublattice are given by a similar expression. The next-nearest-neighbor Ising interaction is now given by

$$H_{M2} = -zz^* S^2 J_2 \sum_{ij} il \left(\frac{P_{ij}^{\alpha\beta} P_{ji}^{\alpha\beta}}{n_j} + \frac{P_{ij}^{\beta\alpha} P_{ji}^{\beta\alpha}}{n_j} \right), \quad (2.11)$$

where z^* is the number of next-nearest neighbors, e.g., $z^* = 6$ for a bcc lattice. We are not interested in discussing spin-disorder-quenched phases, e.g., a spin glass, and for that reason we choose this interaction to be ferromagnetic. In this way J_2 aligns the spins of the same sublattice.

The free energy of the system is then given by

$$\mathcal{F} = H_c + H_{M1} + H_{M2} - TS \quad (2.12)$$

which must be minimized with respect to the $P_{ij}^{\alpha\beta}$, subject to the constraints (2.1) and (2.3). Note that the free energy is invariant under the simultaneous inversion of all the spins in one of the sublattices and a change in the sign of J_1 .

III. RESULTS

In this section we present the results obtained by minimizing the free energy (2.12) with respect to the $P_{ij}^{\alpha\beta}$.

A. Phase diagram at $T = 0$

At $T = 0$ K we have to minimize the internal energy of the system. Since the free energy of the system is invariant under a simultaneous change in the sign of J_1 and inversion of all the spins in one of the sublattices, it is sufficient to discuss the case $J_1 > 0$ only. We have to distinguish the two cases $x = \frac{1}{3}$ (Sm_3S_4) and $x = \frac{2}{3}$ (Eu_3S_4), which correspond to different spin concentrations. For $J_1 > 0$ there are two possible states: a charge-ordered ferromagnetic state (OF) and a segregated ferromagnetic state (SF), in which the ions with

the same valence are clustered.

The boundaries between the phases are given by

$$J_1 = 0, \quad 4U = S^2 |J_1| + \frac{2}{3} z^* S^2 J_2 \quad (3.1)$$

for both systems, $x = \frac{1}{3}$ and $x = \frac{2}{3}$. The phase diagram is shown in Fig. 1 and the states characterized by the nonvanishing pair probabilities are the following:

(1) Concentrated spin system, $x = \frac{1}{3}$ (Sm_3S_4).

OF: ferromagnetic charge ordered $P_{++}^{\alpha\beta} = \frac{1}{3}$, $P_{+0}^{\alpha\beta} = \frac{2}{3}$;

SF: segregated ferromagnetic, $P_{++}^{\alpha\beta} = \frac{2}{3}$, $P_{00}^{\alpha\beta} = \frac{1}{3}$;

OAF: antiferromagnetic charge ordered, $P_{+-}^{\alpha\beta} = \frac{1}{3}$, $P_{+0}^{\alpha\beta} = \frac{2}{3}$;

SAF: segregated antiferromagnetic, $P_{00}^{\alpha\beta} = \frac{1}{3}$, $P_{+-}^{\alpha\beta} = \frac{2}{3}$.

The last two states are obtained from the first two states by inverting the spins in the β sublattice.

(2) Diluted spin system, $x = \frac{2}{3}$ (Eu_3S_4).

OF: ferromagnetic charge ordered, $P_{00}^{\alpha\beta} = \frac{1}{3}$, $P_{0+}^{\alpha\beta} = \frac{2}{3}$;

SF: segregated ferromagnetic, $P_{++}^{\alpha\beta} = \frac{1}{3}$, $P_{00}^{\alpha\beta} = \frac{2}{3}$.

These states are obtained from the corresponding ones for $x = \frac{1}{3}$ by interchanging the alloy components 0 and +.

OF: ferromagnetic charge ordered $P_{00}^{\alpha\beta} = \frac{1}{3}$, $P_{0-}^{\alpha\beta} = \frac{2}{3}$;

SAF: segregated antiferromagnetic $P_{+-}^{\alpha\beta} = \frac{1}{3}$, $P_{00}^{\alpha\beta} = \frac{2}{3}$.

Here again the spins of the β sublattice were reversed. Note that there is no antiferromagnetic charge-ordered phase for spin-diluted systems. It should be mentioned that in this case if $J_2 = 0$ the ordered phases are paramagnetic.

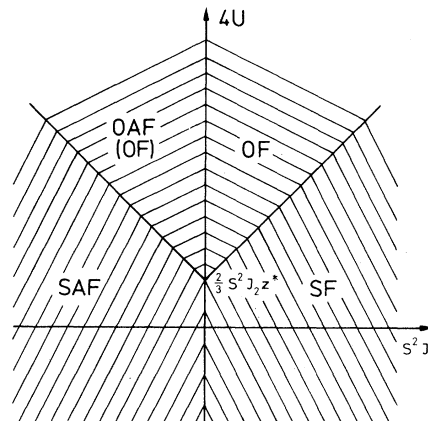


FIG. 1. Ground-state phase diagram. The possible phases are ordered ferromagnetic (OF), segregated ferromagnetic (SF), segregated antiferromagnetic (SAF), and ordered antiferromagnetic (OAF). Notice that OAF cannot exist for a spin-diluted system.

B. Transition temperatures

In general the system undergoes two phase transitions as a function of temperature, corresponding to charge (chemical) and magnetic ordering, respectively. We assume that the charge interaction U is much larger than the Ising spin interactions J_1 and J_2 . We consider only the case of a repulsive U . The charge-ordering temperature of the system is therefore much higher than the Curie or Néel temperature.

In order to calculate the charge-ordering temperature we set then

$$P_{++}^{\alpha\beta} = P_{+-}^{\alpha\beta} = P_{-+}^{\alpha\beta} = P_{--}^{\alpha\beta}, \quad P_{+0}^{\alpha\beta} = P_{-0}^{\alpha\beta}, \quad P_{0+}^{\alpha\beta} = P_{0-}^{\alpha\beta} \quad (3.2)$$

such that the free energy for a given x is only a function of the short-range- and long-range-order parameters σ and η . We find that $\eta=0$ for temperatures higher than the critical temperature T_{CO} , given by¹²

$$T_{CO} = 8U / \ln \left(\frac{x(1-x)z^2}{(z-1-xz)(zx-1)} \right). \quad (3.3)$$

The critical temperature is, of course, the same for $x = \frac{1}{3}$ as for $x = \frac{2}{3}$. The short-range-order parameter at the critical temperature is given by¹²

$$\sigma_{CO} = -1/(z-1) \quad (3.4)$$

independent of the concentration x .

In order to calculate the magnetic transition temperature we have to distinguish between the spin-concentrated and spin-diluted systems. From our previous analysis it is clear that the transition temperature cannot depend on the sign of J_1 . We assume that the magnetic critical temperature T_{CM} is so small that the system is already completely charge ordered. Let us consider the spin-diluted case first. For $x = \frac{2}{3}$ we have that

$$P_{00}^{\alpha\beta} = \frac{1}{3}, \quad P_{+0}^{\alpha\beta} + P_{-0}^{\alpha\beta} = \frac{2}{3}, \quad (3.5)$$

and all others vanish. Hence we have only one order parameter which is long ranged. The transition temperature is then easily obtained:

$$T_{CM} = \frac{8}{3} z z^* S^2 J_2, \quad x = \frac{2}{3}. \quad (3.6)$$

Note that T_{CM} is independent of J_1 , since the probability of finding two neighboring ions with spin is zero.

The case of the spin-concentrated system is more complicated. For $x = \frac{1}{3}$ we have that

$$P_{++}^{\alpha\beta} + P_{+-}^{\alpha\beta} + P_{-+}^{\alpha\beta} + P_{--}^{\alpha\beta} = \frac{1}{3}, \quad P_{+0}^{\alpha\beta} + P_{-0}^{\alpha\beta} = \frac{2}{3} \quad (3.7)$$

and all others are zero. There are four degrees of freedom in the system corresponding to one short-range-order parameter given by

$$\frac{1}{3}\sigma_M \equiv P_{++}^{\alpha\beta} + P_{--}^{\alpha\beta} - P_{+-}^{\alpha\beta} - P_{-+}^{\alpha\beta} \quad (3.8)$$

and three long-range-order parameters, namely, the two sublattice magnetizations and

$$\frac{2}{3}\xi \equiv P_{+0}^{\alpha\beta} - P_{-0}^{\alpha\beta}. \quad (3.9)$$

The free energy is now expanded up to second order in the long-range-order parameters and minimized with respect to them. This yields an homogeneous system of three equations with three unknowns. There is a nontrivial solution only if the determinant vanishes. This yields one relation for $T_{CM}(\sigma_{CM})$; a second relationship is given by

$$\frac{\partial \mathcal{F}}{\partial \sigma_M} = -\frac{1}{3} z S^2 J_1 - \frac{8}{3} z z^* S^2 J_2 \sigma_M + \frac{Tz}{12} \ln \frac{1+\sigma_M}{1-\sigma_M} = 0 \quad (3.10)$$

which is valid for $T \geq T_{CM}$. The critical temperature and the short-range-order parameter are obtained by solving simultaneously these two relations. The critical temperature as a function of J_1 is shown in Fig. 2.

For $U \gg S^2 |J_1| \gg z^* S^2 J_2$ we obtain that

$$\sigma_{CM} = \sqrt{3}/(z-1) \quad (3.11)$$

and

$$T_{CM} = 4S^2 |J_1| / \ln \left(\frac{z-1+\sqrt{3}}{z-1-\sqrt{3}} \right), \quad (3.12)$$

i. e., T_{CM} is proportional to $|J_1|$, as can be seen in Fig. 2.

C. The conductivity of Sm_3S_4 near the order-disorder transition

As mentioned in the Introduction, the electrical conductivity is due to a thermally activated hopping as given by (1.1). The data for Sm_3S_4 shows a

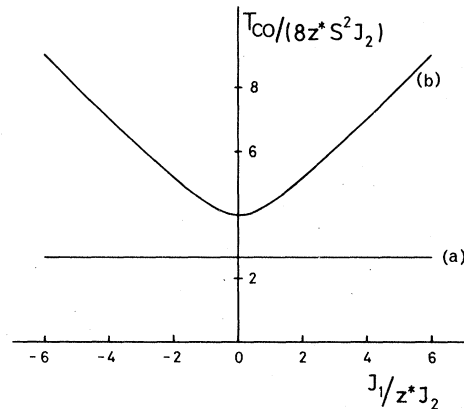


FIG. 2. Critical temperatures for magnetic ordering as a function of nearest-neighbor coupling for a charge-ordered system: (a) the spin-diluted and (b) the spin-concentrated case.

change in the activation energy² at 125 K. A possible explanation for this change is a charge-ordering transition. We assume that the conductivity is proportional to the available Sm^{2+} - Sm^{3+} pairs in the system, since these are the only bonds that contribute to the transport. With the conditions (2.1), (2.3b), and (3.2) our system depends only on the short- and long-range-order parameters, defined in (2.6) and (2.7). The probability of finding a pair with unlike charges depends only on the short-range-order parameter

$$P_{2^+3^+} = 2x(1-x)(1-\sigma) \quad (3.13)$$

whose equilibrium value is obtained by minimization of the free energy with respect to σ and η . Close to the order-disorder transition we obtain the following expression for σ :

$$\sigma - \sigma_{\text{CO}} = \frac{8U}{T_{\text{CO}}^2} \frac{(T - T_{\text{CO}})}{A + B\Theta(T_{\text{CO}} - T)}, \quad (3.14)$$

where $\Theta(x)$ is the step function, which is one for $x > 0$ and zero for $x < 0$, and T_{CO} and σ_{CO} are given by (3.3) and (3.4), respectively. The constants A and B are defined by

$$A = (z-1) \left(\frac{x}{z(1-x)-1} + \frac{1-x}{zx-1} + \frac{2}{z} \right), \quad (3.15)$$

$$B = 3 \left(\frac{z-1}{z} \right)^3 / \left[(1-x)^3 + x^3 - \left(1 - \frac{1}{z} \right)^2 \right]. \quad (3.16)$$

We see that the slope of σ as a function of temperature changes at T_{CO} due to the onset of the long-range order.

The variation of $P_{2^+3^+}$ with the temperature is shown in Fig. 3 together with some of the conductivity data² of Sm_3S_4 . The interaction strength U has been determined from the critical temperature $T_{\text{CO}} = 125$ K, and the high-temperature data has been matched to fix the activation energy ΔE , Eq. (1.1). The rest of the figure follows without adjusting further parameters and is in good agree-

ment with the experiment.

The high-temperature activation energy cannot be calculated easily. Inelastic light scattering experiments³ revealed the existence of an anomalous phonon mode associated with the valence fluctuation in Eu_3S_4 . It corresponds to a zone-boundary mode in which the S atoms vibrate, while the R ions remain essentially fixed. The hopping frequency ν_0 in (1.1) is also of the order of optical phonon energies. Hence lattice vibrations should not be neglected in estimations of the hopping integral, i. e., the activation energy.

D. Discontinuity of the specific heat at the order-disorder transition

The onset of long-range order induces a jump in the specific heat at T_{CO} . We consider here only the electronic contributions due to a feasible lattice distortion.¹³ In order to obtain the specific-heat jump we expand the free energy in powers of η up to fourth order and minimize with respect to σ and η . The specific heat is given by the second derivative of \mathcal{F} with respect to the temperature which yields

$$C = 32zx(1-x)(U/T_{\text{CO}})^2 / [A + B\Theta(T_{\text{CO}} - T)] + O(T - T_{\text{CO}}), \quad (3.17)$$

where A and B are defined by (3.15) and (3.16).

The discontinuity is then given by

$$\Delta C = -32zx(1-x)(U/T_{\text{CO}})^2 \frac{B}{A(A+B)}. \quad (3.18)$$

For $x = \frac{1}{3}$ or $x = \frac{2}{3}$ we obtain

$$\Delta C = \frac{64}{81} \left(\frac{U}{T_{\text{CO}}} \right)^2 \frac{z^2(z-3)^2(2z-3)^2}{(z-1)(z-2)(z^2-3z+3)}. \quad (3.19)$$

IV. SUMMARY AND CONCLUSIONS

We have presented a model for inhomogeneous semiconducting mixed-valence compounds, in

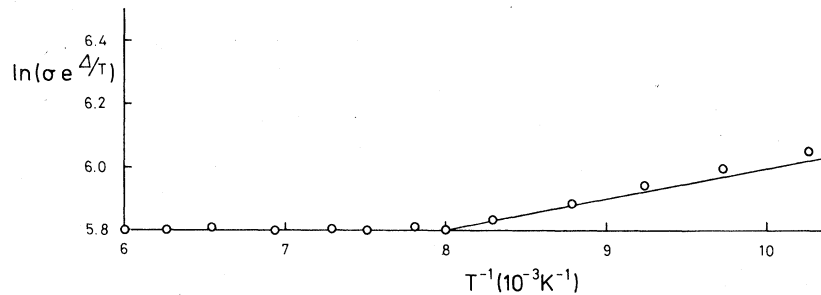


FIG. 3. Conductivity $\sigma (\Omega^{-1} \text{cm}^{-1})$ of Sm_3S_4 as a function of the inverse temperature. The experimental data are taken from Ref. 2. Only the critical temperature $T_{\text{CO}} = 125$ K and the high-temperature activation energy $\Delta E = 0.142$ eV are fitted to the experimental data; the rest of the curve follows from the model without adjusting any further parameters.

which the dynamics of the $4f$ levels is neglected. The system was treated as a ternary alloy within the Bethe-Peierls approximation; the alloy components being nonmagnetic ions and magnetic ions with spin up and down, respectively. We considered a charge interaction between neighboring ions and Ising-spin interaction between nearest and next-nearest neighbors. In Sec. III we calculated the ground-state phase diagram, the critical temperatures, and the behavior near the order-disorder transition.

We have focused our attention on the systems Sm_3S_4 and Eu_3S_4 , which are expected to behave similarly for temperatures far above the magnetic ordering temperature. The electrical-conductivity data² for Sm_3S_4 revealed an anomaly in the hopping activation energy of the $4f$ electrons at 125 K. This change in the activation energy can be explained in terms of an order-disorder transition as is shown in Fig. 3. At the order-disorder transition the specific heat should have a discontinuity. A measurement of the specific heat should be of interest. The low-temperature specific heat is dominated by the lattice vibrations, whereas at higher temperatures the electronic disorder is expected to play an important role. Since electrons and phonons are coupled as found by inelastic light scattering,³ the order-disorder transition might be accompanied by a lattice distortion. The strength of the distortion may be estimated by comparing $T_{CO} = 125$ K with the energy separation² between the $4f^6$ and $4f^5$ states of Sm which is $\mu = 4.5$ eV. The latter energy should be of the order of the "local deformation energy" due to the difference in size of the Sm^{2+} and Sm^{3+} ions. We ex-

pect the lattice distortion to be of the order of

$$\delta \sim T_{CO}/\mu \sim 0.2-0.3\% \quad (4.1)$$

which is in agreement with the lattice distortion determined¹³ for Eu_3S_4 of about 0.4%.

At low temperatures we expect the system to order magnetically. This is in agreement with some of the experimental data.^{6,7} Here we have to distinguish between the Sm and the Eu compounds, since they correspond to the spin-concentrated and spin-diluted cases, respectively. The Eu compound cannot order magnetically if only a nearest-neighbor interaction is taken into account.

There are two main mechanisms contributing to the spin interactions¹¹: (a) In the *superexchange* the R ions interact by spin-polarizing the p orbitals of the neighboring anions (S^{2-} ions). The effective interaction is always antiferromagnetic and decreases exponentially with the distance. (b) In the *indirect exchange* the $4f$ electrons are virtually excited into the $5d$ band and mediate in this way an effective interaction between the R ions. This mechanism is always ferromagnetic and also short ranged.

The short rangeness of the interactions justifies the consideration of only nearest- and next-nearest-neighbor interactions in a bcc lattice. We have two competing mechanisms, one being antiferromagnetic, the other ferromagnetic. Since the Sm^{2+} ion is nonmagnetic we expect the indirect exchange to be less effective for Sm_3S_4 than for Eu_3S_4 where Eu^{2+} has a $S = \frac{7}{2}$ ground state. This simple argument may be the explanation for the antiferromagnetic ordering of Sm_3S_4 and the ferromagnetic ordering of Eu_3S_4 .

*Present address: Departamento de Física, Centro de Investigación y Estudios Avanzados del I. P. N., Apdo. Postal 14-740, México 14, D. F.

¹J. M. Robinson, Phys. Rep. **51**, 1 (1979).

²B. Batlogg, E. Kaldis, A. Schlegel, G. von Schulthess, and P. Wachter, Solid State Commun. **19**, 673 (1976).

³J. Vitins and P. Wachter, Physica **89B**, 234 (1977).

⁴I. A. Smirnov, L. S. Parfen'eva, V. Ya Khusnutdinova, and V. M. Sergeeva, Fiz. Tverd. Tela **14**, 2783 (1972) [Sov. Phys.—Solid State **14**, 2412 (1972)].

⁵O. Berkooz, M. Malamud, and S. Shtrikman, Solid State Commun. **6**, 185 (1968).

⁶E. Görrlich, H. U. Hryniewicz, R. Kmieć, K. Łatka,

and K. Tomala, Phys. Status Solidi B **64**, K147 (1974).

⁷P. Wachter, Phys. Lett. **58A**, 484 (1976).

⁸M. Escorne, A. Ghazali, P. Leroux Hugon, and I. A. Smirnov, Phys. Lett. **56A**, 475 (1976).

⁹C. Domb, Adv. Phys. **9**, 149 (1960), see pp. 251–252.

¹⁰P. Schlottmann, J. Magn. Mater. **13**, 189 (1979).

¹¹P. W. Anderson, in *Magnetism*, edited by G. T. Rado and H. Suhl (Academic, New York, 1963), Vol. I, p. 25.

¹²J. L. Morán-López and L. M. Falicov, Phys. Rev. B **18**, 2542 (1978).

¹³H. H. Davis, I. Bransky and N. M. Tallan, J. Less-Common Met. **22**, 193 (1970).